ACS Partner Journal

CHEM & BIO ENGINEERING

pubs.acs.org/ChemBioEng

Article

Robust Two-Dimensional Hydrogen-Bonded Organic Framework for Efficient Separation of C1−C3 Alkanes

Published as part of Chem & Bio Engineering virtual special issue "Advanced Separation Materials and Processes".

Yunzhe Zhou, Yongqin Zhu, Danhua Song, Zhenyu Ji, Cheng Chen, and Mingyan Wu*

Cite This: *Chem Bio Eng.* 2024, 1, 846−854

Read Online

ACCESS | Metrics & More | Article Recommendations | Supporting Information

ABSTRACT: Separating natural gas to obtain high-quality C1−C3 alkanes is an imperative process for supplying clean energy sources and high valued petrochemical feedstocks. However, developing adsorbents which can efficiently distinguish CH_4, C_2H_6, and C_3H_8 molecules remains challenging. We herein report an ultra-stable layered hydrogen-bonded framework (HOF-NBDA), which features differential affinities and adsorption capacities for CH_4, C_2H_6, and C_3H_8 molecules, respectively. Breakthrough experiments on ternary component gas mixture show that HOF-NBDA can achieve efficient separation of $CH_4/C_2H_6/C_3H_8$ (v/v/v, 85/7.5/7.5). More importantly, HOF-NBDA can realize efficient C_3H_8 recovery from ternary $CH_4/C_2H_6/C_3H_8$ gas mixture. After one cycle of breakthrough, 70.9 $L{\cdot}kg^{-1}$ of high-purity (≥ 99.95%) CH_4 and 54.2 $L{\cdot}kg^{-1}$ of C_3H_8 (purity ≥99.5%) could be obtained. Furthermore, excellent separation performance under different flow rates, temperatures, and humidities could endow HOF-NBDA an ideal adsorbent for the future natural gas purification.

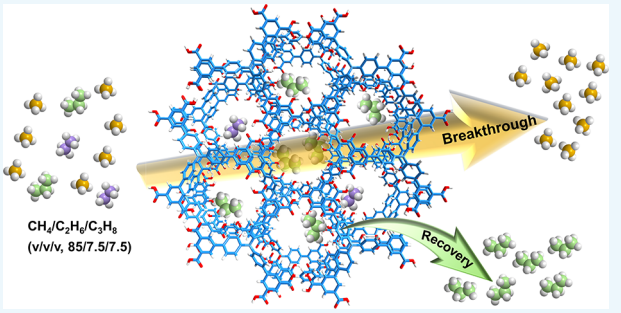

KEYWORDS: *hydrogen-bonded organic framework, two-dimensional structure, gas separation, natural gas, propane recovery*

INTRODUCTION

Presently, human's dependence on fossil energy causes excessive emissions of greenhouse gas especially carbon dioxide (CO_2) and leads to irreversible climate change.[1−5] Thus, new clean energy sources are urgently desired to alleviate this excessive carbon emission. Natural gas is a significant clean energy source that is mainly composed of CH_4 which endows it with a high hydrogen to carbon ratio and high energy density of 55.5 $MJ{\cdot}kg^{-1}$.[6−8] Besides, raw natural gas also contains a small quantity (∼20%) of variable amounts of impurities, such as C_2H_6, C_3H_8, and so forth.[9−13] Among them, C_2H_6 and C_3H_8 are usually used as the feedstocks to produce higher value-added olefins (C_2H_4 and C_3H_6), which are usually used as the building blocks to synthesize polyethylene or polypropylene-based materials.[14−18] Consequently, separating natural gas to obtain high-purity CH_4 and other remaining alkanes is of great importance to realize the efficient utilization of natural gas. Nowadays, the upgrading and purification techniques of light hydrocarbons are mainly achieved by extraction and cryogenic distillation, requiring large energy consumption that does not match the requirements of sustainable development. Recently, adsorptive separation based on porous materials has emerged as an environment-friendly and energy-efficient separation progress and has been considered as an alternative to traditional separation and purification methods.[19−22] Therefore, developing such method to separate natural gas is necessary for alleviating energy consumption.

As for adsorptive separation, adsorbents are considered the most important determinant of adsorptive separation. Considerable research efforts have been contributed to develop excellent adsorbents for light hydrocarbon separation. Adsorbents like zeolites, metal−organic frameworks (MOFs), and porous carbon materials have been intensively developed for industrial gas separation.[23−26] However, as we all know, an ideal adsorbent should not only have high adsorption capacity and selectivity, but also have high stability, easy scalability of synthesis and mild regeneration to realize the application in industrial environment. Therefore, considering the comprehensive factors, previous reports material is difficult to meet the rigorous industrial requirements. And thus, it is necessary

Received: March 13, 2024
Revised: May 17, 2024
Accepted: May 21, 2024
Published: June 4, 2024

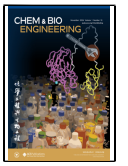

https://doi.org/10.1021/cbe.4c00057
Chem Bio Eng. 2024, 1, 846−854

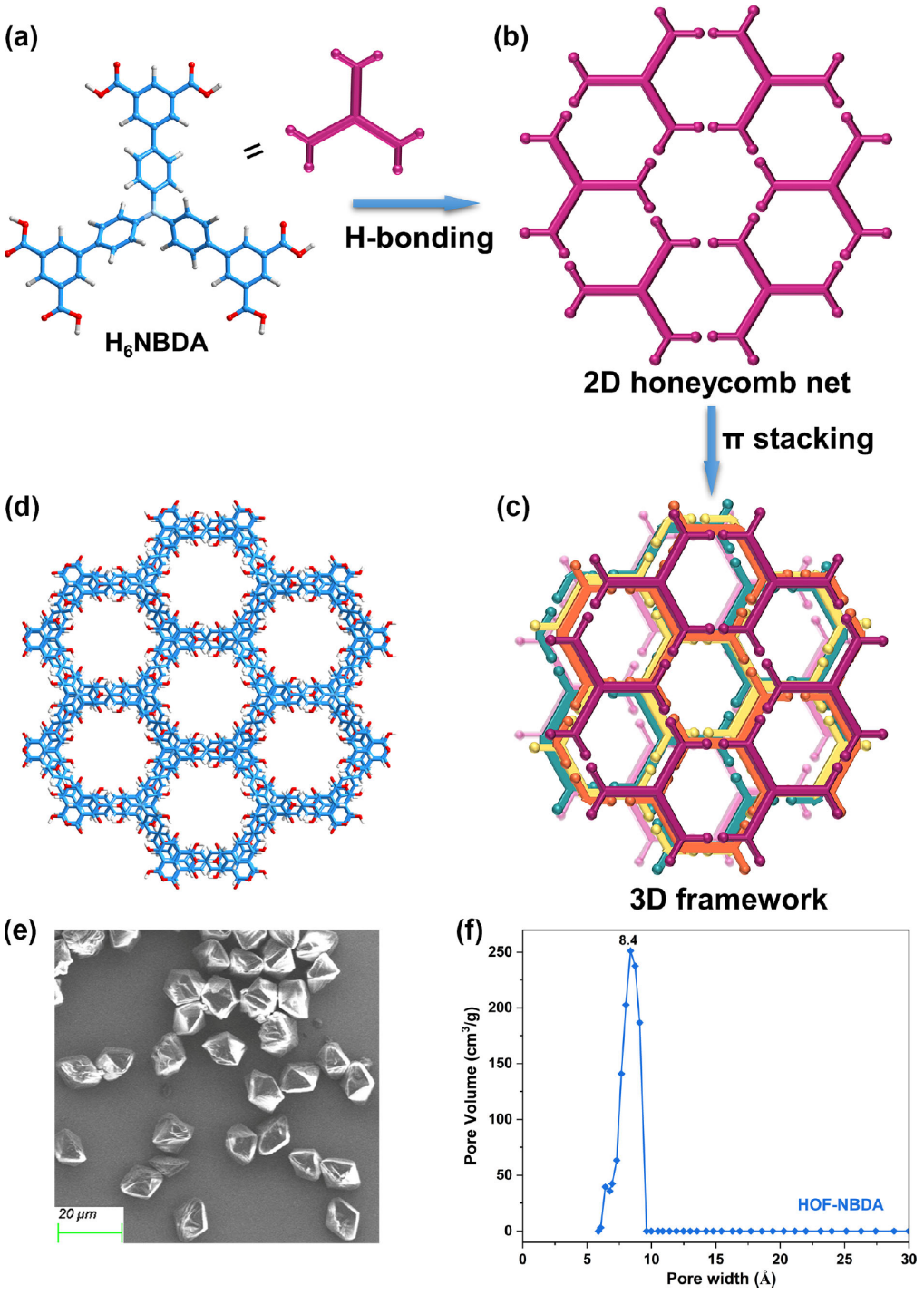

Figure 1. (a) The molecular structure of H_6NBDA. (b) Representation of the two kinds of hexagonal windows and the resulting monolayer network in HOF-NBDA. (c) The layered frameworks are stacked in slippage in an −ABCD− manner without interpenetration. (d) Top viw of 1D channel in the framework. (e) The SEM image and (f) pore size distributions of HOF-NBDA.

to develop more advantageous porous materials to adapt to industrial separation conditions. Hydrogen-bonded organic frameworks (HOFs), which have emerged as a new type of superior porous materials, are generally constructed by discrete organic molecules via intermolecular hydrogen-bonding interactions. Besides, introducing some other supramolecular interactions such as $\pi\cdots\pi$ conjugate can cooperatively endow HOFs with stable structures.[27−29] On the basis of these strategies, a series of robust HOFs with permanent porosity have been successfully constructed to apply for gas separation, such as C_2H_6/C_2H_4, C_2H_2/CO_2, C_2H_2/C_2H_4, C_3H_8/C_3H_6, and so on.[30−33] However, HOFs are rarely an efficient adsorbent for CH_4 purification and C_3H_8 recovery from natural gas.

On the basis of the above considerations, we herein report a hydrogen-bonded organic framework HOF-NBDA, which is created by an organic ligand for a planar hexacarboxylic acid and possesses a two-dimensional graphene-sheet-like structure with a particular −ABCD− staking model. Benefiting from the particularity of its structure and inert pore environment, HOF-

https://doi.org/10.1021/cbe.4c00057
Chem Bio Eng. 2024, 1, 846−854

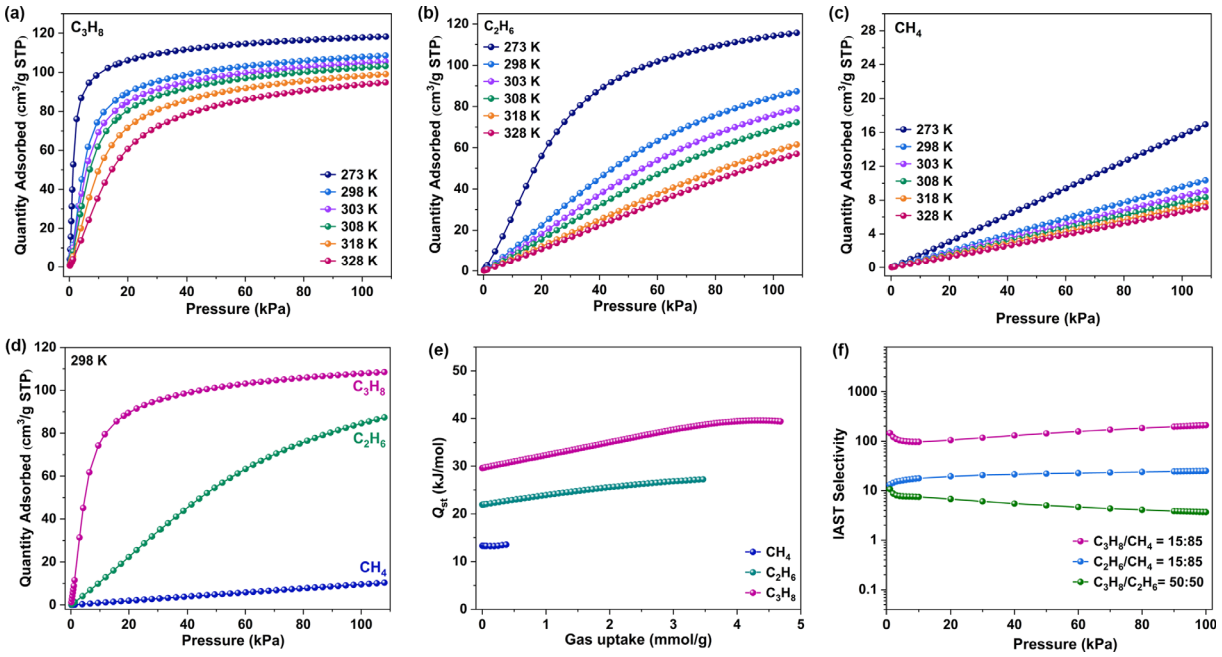

Figure 2. (a–c) Single-component adsorption isotherms of C_3H_8, C_2H_6, and CH_4 at 273–323 K. (d) The comparison of adsorption isotherms of C_3H_8, C_2H_6, and CH_4 at 298 K. (e) The Q_{st} of HOF-NBDA for CH_4, C_2H_6, and C_3H_8. (f) IAST selectivities of HOF-NBDA for C_3H_8/CH_4, C_2H_6/CH_4, and C_3H_8/C_2H_6.

NBDA exhibits a large difference between the affinity of C_3H_8, C_2H_6, and CH_4. At 298 K and 1 bar, HOF-NBDA shows a high uptake of C_3H_8 (108.5 $cm^3 \cdot g^{-1}$), a moderate uptake of C_2H_6 (87.3 $cm^3 \cdot g^{-1}$) and a relatively low adsorption capacity of CH_4 (10.3 $cm^3 \cdot g^{-1}$). Due to the large difference in C_3H_8, C_2H_4, and CH_4 uptakes, HOF-NBDA shows excellent performance for $CH_4/C_2H_6/C_3H_8$ (v/v/v, 85/7.5/7.5) gas mixture separation. After one cycle of the separation and desorption experiment at ambient condition, 70.9 $L \cdot kg^{-1}$ of high-purity ($\geq$ 99.95%) CH_4 and 54.2 $L \cdot kg^{-1}$ of C_3H_8 with high-purity ($\geq$ 99.5%) could be obtained. In addition, HOF-NBDA can retain excellent $CH_4/C_2H_6/C_3H_8$ separation performance at different gas flow rates, temperatures, and relative humidity conditions, which is rarely seen in the gas separation materials. Furthermore, theoretical simulations reveal that the two-dimensional structure and inert surfaces of HOF-NBDA supply much more supramolecular interactions with C_3H_8 than C_2H_4 and CH_4, which plays the key role in markable $CH_4/C_2H_6/C_3H_8$ separation performance.

RESULTS AND DISCUSSION

Crystal Structure of HOF-NBDA. Yellow crystals of HOF-NBDA can be obtained by simple solution diffusion method (see Supporting Information, SI). In the crystal structure of HOF-NBDA, three external benzene rings with *m*-benzenedicarboxylate acids coexist in one plane as the central triphenylamine, presenting H_6NBDA a planar conformation with C_3 symmetry (Figure 1a). Each H_6NBDA molecule is connected with six neighboring molecules through six pairs of O–H···O hydrogen bonds, extending into an irregular honeycomb layer with two kinds of hexagonal cavities about 14.4 × 14.3 $Å^2$ and 10.1 × 12.0 $Å^2$ (Figure 1b). Adjacent 2D layers are packing together through discontinuous $\pi \cdots \pi$ interactions, which results in a porous framework with 1D channel along the *a*-axis with the size of ca. 8.4 Å (calculated by Zeo++ package)[34] (Figure 1c,d).

Gas Adsorption Experiments. The phase purity of HOF-NBDA was verified by powder X-ray diffraction (PXRD) patterns and scanning electron microscopy (SEM) (Figure 1e). N_2 adsorption experiment at 77 K revealed that HOF-NBDA exhibits a typically reversible type-I type and the calculated BET surface area is 965 $m^2 \cdot g^{-1}$.[17] The calculated pore size is 8.4 Å (Figure 1f), which matchs well with the value obtained from the crystal structure. Motivated by the suitable pore size of and unique layered structure of HOF-NBDA, we have conducted single-component adsorption isotherms for C_3H_8, C_2H_6, and CH_4 in the range of 273 K to 328 K, respectively. As shown in Figure 2a–d and Figure S3, the storage capacity of C_3H_8 is noticeably higher than those of C_2H_6 and CH_4 at the 273–328 K. Besides, due to the negligible adsorption of CH_4, the uptake of C_2H_6 for HOF-NBDA is also higher than CH_4. The uptakes for these three light hydrocarbons follows the squence of $C_3H_8 > C_2H_6 > CH_4$, which confirms that HOF-NBDA favorably adsorbs C_3H_8 and C_2H_6 molecules over CH_4. At 298 K and 100 kPa, the storage capacity of C_3H_8 and C_2H_6 are high up to 108.5 $cm^3 \cdot g^{-1}$ and 87.3 $cm^3 \cdot g^{-1}$, respectively, while the amount of CH_4 adsorbed by HOF-NBDA is only 10.3 $cm^3 \cdot g^{-1}$, performing that the gas uptake increases with the prolongation of the carbon chain. It is worth noticing that the adsorption isotherm of C_3H_8 displays a steep increase in the range of low pressure. Therefore, it is suspected that the C_3H_8 molecules interacts more strongly with the framework than C_2H_6 and CH_4, which is also reported in the previous research.[35–37] More importantly, at 5 kPa, the uptake of C_3H_8 can reach 52.2 $cm^3 \cdot g^{-1}$, which is much higher than the uptake of C_2H_6 (ca. 5.9 $cm^3 \cdot g^{-1}$) and CH_4 (ca. 0.5 $cm^3 \cdot g^{-1}$) at the same pressure. The C_3H_8 uptake at low pressure (5 kPa) is slightly lower than these adsorbents with ultra-high C_3H_8 uptakes, such as Fe-pyz (61.4 $cm^3 \cdot g^{-1}$) and Co-pyz (63.7 $cm^3 \cdot g^{-1}$)[38] (Table S3), but is much higher than HOF-ZJU-201a (49.9 $cm^3 \cdot g^{-1}$),[39] MIL-142A (41.2 $cm^3 \cdot g^{-1}$),[40] Co-MOF (36.6 $cm^3 \cdot g^{-1}$),[13] UiO-67 (22.4 $cm^3 \cdot g^{-1}$),[41] and SDMOF-3

https://doi.org/10.1021/cbe.4c00057
Chem Bio Eng. 2024, 1, 846–854

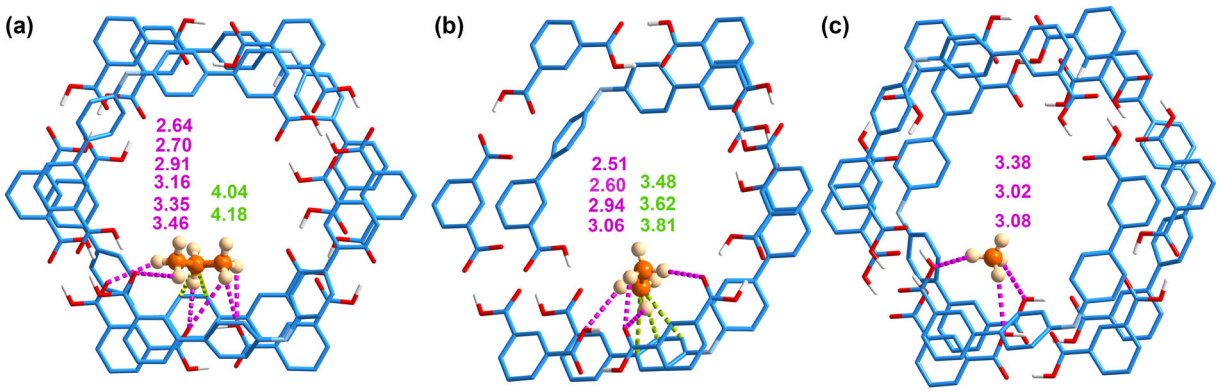

Figure 3. Adsorption configurations on HOF-NBDA for (a) C_3H_8, (b) C_2H_6, and (c) CH_4. C−H···π interactions are represented by green dashed lines, whereas the C−H···O hydrogen bonds are represented by pink dashed lines. For C−H···π interactions, the distances represent the C···C separations, which for C−H···O hydrogen bonds the distances represent the H···O separations. All distances are given in angstrom unit.

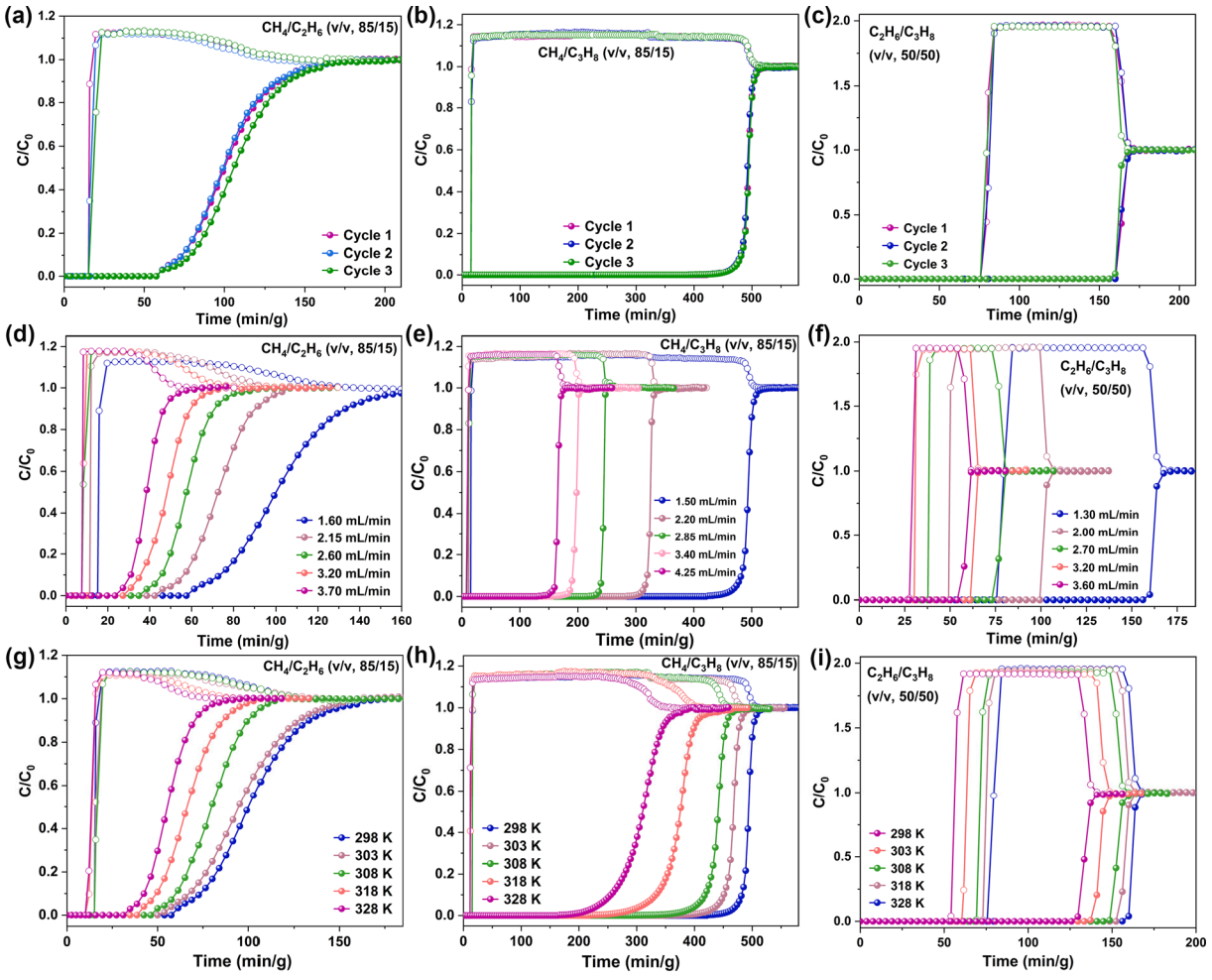

Figure 4. Breakthrough curves of binary mixture through the fixed bed packed with HOF-NBDA. Three-cycles tests at 298 K for (a) CH_4/C_2H_6 (v/v = 85/15, 1.60 mL·min^{-1}), (b) CH_4/C_3H_8 (v/v = 85/15, 1.50 mL·min^{-1}) and (c) C_2H_6/C_3H_8 (v/v = 50/50, 1.30 mL·min^{-1}) gas mixture. The breakthrough curves with different flow rates 298 K for (d) CH_4/C_2H_6, (e) CH_4/C_3H_8, and (f) C_2H_6/C_3H_8. The breakthrough curves at different temperatures for (g) CH_4/C_2H_6 (1.60 mL·min^{-1}), (h) CH_4/C_3H_8 (1.50 mL·min^{-1}), and (i) C_2H_6/C_3H_8 (1.30 mL·min^{-1}).

(36.1 cm^3·g^{-1}).[42] The remarkable differences between these light hydrocarbons predict that HOF-NBDA has great potential for separating these gases mixture.

In order to further investigate the interactions between the gas and framework, the isosteric heats of adsorption (Q_{st}) for C_3H_8, C_2H_6, and CH_4 are calculated based on the mathematical analysis of the adsorption isotherms. After fitting the adsorption curves of 273, 298, and 303 K, the Q_{st} values could be obtained and described in Figure 2e. The Q_{st} value of C_3H_8 at zero loading is 29.6 kJ·mol^{-1}, which is higher than that of C_2H_6 (21.9 kJ·mol^{-1}) and far more than that of CH_4 (13.3 kJ·mol^{-1}). These results indicate that HOF-NBDA can

https://doi.org/10.1021/cbe.4c00057
Chem Bio Eng. 2024, 1, 846−854

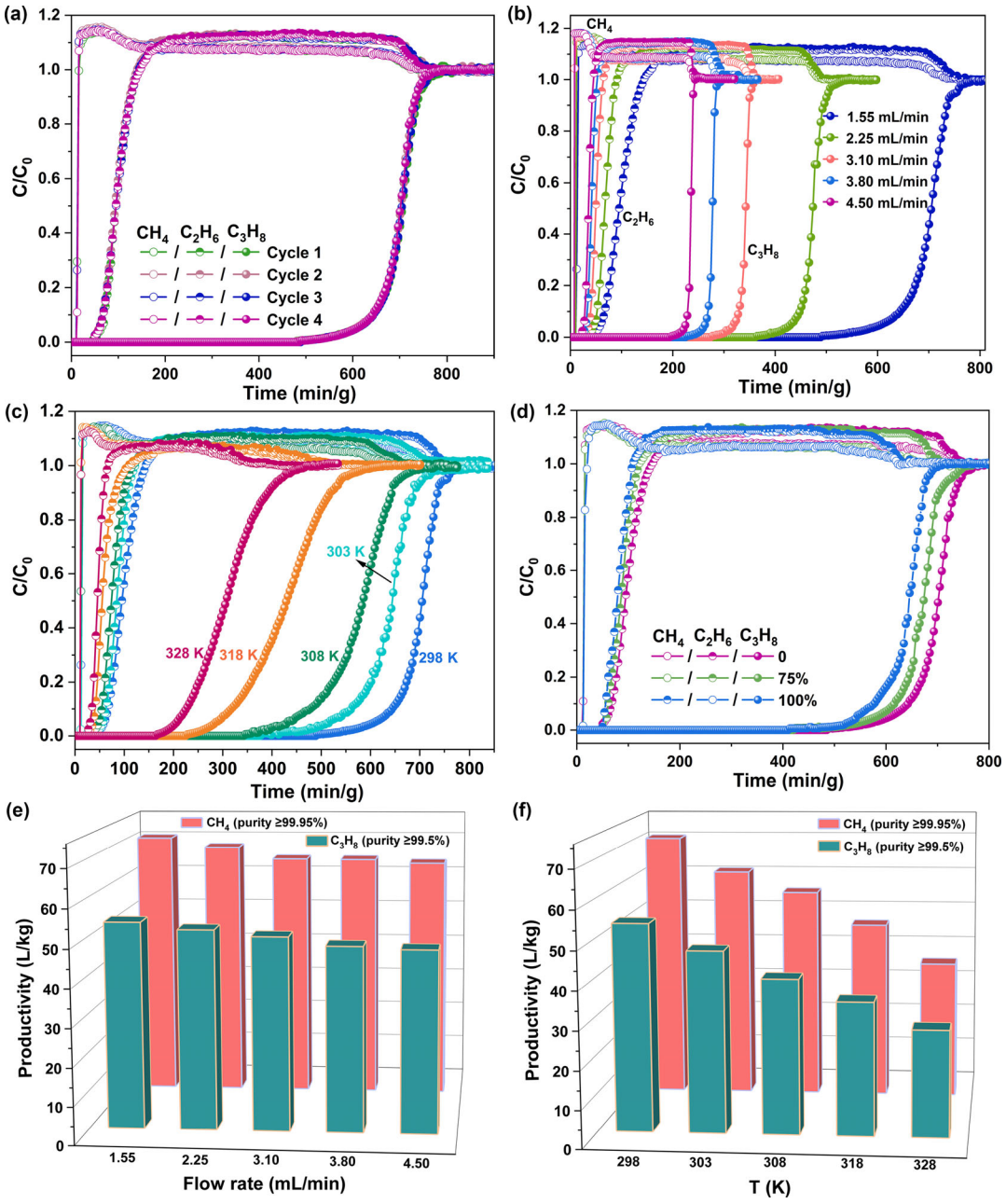

Figure 5. Breakthrough experiments of HOF-NBDA for $CH_4/C_2H_6/C_3H_8$ (v/v/v = 85/7.5/7.5). (a) Cycle tests at 298 K with the gas flow rate of 1.55 mL·min^{-1}. (b) The breakthrough curves with different flow rates at 298 K. (c) The breakthrough curves with flow rate of 1.55 mL·min^{-1} at different temperatures. (d) The breakthrough experiments of HOF-NBDA at different relative humidities with gas flow rate of 1.55 mL·min^{-1}. (e) The productivities for CH_4 under different flow rates at 298 K. (f) The productivities for CH_4 at different temperatures with flow rate of 1.55 mL·min^{-1}. (Figure 4e,f is drawn according to the data in Tables S1 and S2.).

effectively differentiate CH_4, C_2H_6, and C_3H_8, and has great potential in CH_4 purification and separation from ternary mixed gas. Meanwhile, the Q_{st} value for C_3H_8 is moderately high and much lower than UiO-67 (47.5 kJ·mol^{-1}),[40] Cu-IPA (43.9 kJ·mol^{-1}),[43] DMOF-Cl (36 kJ·mol^{-1}),[44] and Ni-MOF (39.6 kJ·mol^{-1}).[35] Such a moderate Q_{st} endows the preferential C_3H_8 adsorption as well as facile recovery of C_3H_8 under mild conditions with a low energy input during the desorption process. Moreover, to further evaluate the separation potential of HOF-NBDA for CH_4, C_2H_6, and C_3H_8, ideal adsorbed solution theory (IAST) is employed to calculate the selectivity for the gas mixtures of C_3H_8/CH_4 (v/v, 15/85), C_2H_6/CH_4 (v/v, 15/85), and C_3H_8/C_2H_6 (v/v, 50/50) at 298 K and 100 kPa. As depicted in Figure 2f, the selectivity of CH_4/C_3H_8, CH_4/C_2H_6, and C_2H_6/C_3H_8 can reach 210.1, 25.0, and 3.7, respectively. Specifically, the CH_4/C_3H_8 (85:15) IAST selectivity for HOF-NBDA exceeds that of HOF-ZJU-201a (119),[39] UiO-66 (32.0),[45] Zn-BPZ-SA (65.7),[46] and SDMOF-3 (49.4),[42] it is lower than that of NIIC-20-Et (1110),[47] Co-MOF (290),[13] MIL-142A (1300),[40] and BSF-1 (353).[48] The above result also indicates that HOF-NBDA has great potential for $CH_4/C_2H_6/C_3H_8$ separation.

Separation Mechanism. For comprehensive insight into the selective adsorption mechanism, the adsorption sites and bonding potentials for C_3H_8, C_2H_6, and CH_4 with HOF-NBDA were simulated. We found that for all three gas

https://doi.org/10.1021/cbe.4c00057
Chem Bio Eng. 2024, 1, 846−854

molecules, the primary adsorption sites are located at the corners of the hexagonal channel-like pores. The lowest-energy adsorption site was calculated and is shown in Figure 3. The calculated binding energies follow the order of C_3H_8 (50.2 kJ·mol^{-1}) > C_2H_6 (35.8 kJ·mol^{-1}) > CH_4 (24.9 kJ·mol^{-1}) for HOF-NBDA, which matches well with the experimental Q_{st} at zero coverage. As shown in Figure 3a, multiple supramolecular interactions are observed between the C_3H_8 molecule and the framework. Each C_3H_8 molecule is hydrogen bonded to four carboxylate O atoms through six C−H···O interactions with the O···H distances of 2.64−3.46 Å. In addition, the C_3H_8 molecule also interacts with the adjacent benzene ring through two C−H···π interactions (corresponding C···C separations, 4.04 and 4.18 Å, respectively). For C_2H_6, there are four C−H···O interactions (2.51−3.06 Å), and three C−H···π interactions (3.48, 3.62, and 3.81 Å, respectively) (Figure 3b). In contrast, CH_4 exhibits only three weak C−H···O interactions (H···O, 3.02−3.38 Å) (Figure 3c). Evidently, due to the more H atoms and larger molecular size of C_3H_8, the C_3H_8 molecule exhibits much more supramolecular interactions with the framework, resulting in the strongest binding affinity. All the above results are well consistent with the experimental observations, which can visually elucidate the adsorption and separation phenomenon on natural gas mixtures.

Selective Separation of Binary Mixtures. To verify the actual separation ability of HOF-NBDA, experimental breakthrough studies were performed in a packed column of activated HOF-NBDA samples with flow feed gases under different conditions. Firstly, binary CH_4/C_2H_6 (v/v = 85/15, total flow = 1.60 mL·min^{-1}), CH_4/C_3H_8 (v/v = 85/15, total flow = 1.50 mL·min^{-1}) and C_2H_6/C_3H_8 (v/v = 50/50, total flow = 1.30 mL·min^{-1}) mixtures were employed for testing the separation ability for HOF-NBDA. As anticipated, HOF-NBDA can realize efficient separation of CH_4/C_2H_6, CH_4/C_3H_8, and C_2H_6/C_3H_8 mixtures. As demonstrated in Figure 4a,b, CH_4 gases could flow out at first when the feeding gases are CH_4/C_2H_6 and CH_4/C_3H_8, while the C_2H_6 or C_3H_8 gas can be detected a long time later. The retention times could reach 42.4 and 376.2 min, respectively, for CH_4/C_2H_6 and CH_4/C_3H_8 under 298 K, corresponding the productivities of high-purity CH_4 (≥99.95%) are 69.9 L·kg^{-1} and 99.6 L·kg^{-1}. When the gas mixture is changed into C_2H_6/C_3H_8, it can be seen that HOF-NBDA could also achieve effective separation of the two components, and the interval between C_2H_6 and C_3H_8 is 84.3 min (Figure 3c). Subsequently, cycling tests were conducted to illustrate the reusability of HOF-NBDA. As shown in Figure 3a−c, after three circles of breakthough experiments for CH_4/C_2H_6, CH_4/C_3H_8, and C_2H_6/C_3H_8, there were no significant changes in the separation curves, indicating HOF-NBDA possesses excellent cyclic stability. In order to further verify that HOF-NBDA can work well under the actual conditions, separation experiments under different flow rates and temperatures were also performed. As can be seen from Figures 4d−f and S4−S5, when the gas flow rate gradually increases, there is no significant change in the corresponding gas productivities, indicating that the flow rates had no effect on the separation performance of the HOF-NBDA. In the next, the separation performance of HOF-NBDA was investigated at different temperatures. As shown in Figure 4g−i, although the separation performance would decline in a certain extent as the separation temperature gradually increases. When the temperature reaches 328 K, 35.8 L·kg^{-1} and 51.3 L·kg^{-1} of pure CH_4 could be still obtained respectively from CH_4/C_2H_6 and CH_4/C_3H_8 gas mixtures after one breakthough test (Figures S4 and S5).

Selective Separation of $CH_4/C_2H_6/C_3H_8$ Gas Mixtures. Inspired by superior separation performance of HOF-NBDA for binary gas mixtures, we next employed the ternary $CH_4/C_2H_6/C_3H_8$ (v/v/v, 85/7.5/7.5) mixture with a total flow rate of 1.55 mL·min^{-1} to further evaluate its separation capacity. As anticpated, CH_4 rapidly elutes through the packed column at 10.1 min owing to the weakest interactions, and then C_2H_6 remains in the column for a longer time and is detected after about 30 min (Figure 5a). Whereas C_3H_8 eluted at last being attributed to the strongest adsorbate interation. The difference between the breakthrough times (Δt) for C_2H_6 and C_3H_8 is as long as 438.9 min. Importantly, the productivity of CH_4 (high purity ≥99.95%) harvested from the ternary mixture is estimated as 70.9 L·kg^{-1} (Table S1). Additionally, the recyclability of porous materials is very important in practical applications. As can be seen in Figure 5a, the breakthrough curves after four adsorption cycles are basically the same. At the meantime, the PXRD patterns after breakthrough experiments are also consistent with the simulated ones (Figure S2), indicating HOF-NBDA has excellent stability for $CH_4/C_2H_6/C_3H_8$ mixture separation. To meet more practical application, adsorbent should maintain a good separation performance under the wide range of conditions, including different flow rates and temperatures. As shown in Figure 5b, HOF-NBDA shows an excellent separation performance when the flow rates continuously increased, even up to 4.5 mL·min^{-1}. Furthermore, when the temperature raises to 328 K, the ternary separation performance has no obvious change, and the CH_4 productivity is as high as 27.7 L·kg^{-1} (Figure 5c and Table S2).

In industrial natural gas separation, the feedstock gases contain trace water vapor, which is a huge challenge for the adsorption capacity and septation performance of the materials.[49−51] Very importantly, with the moisture of 100% RH in the gas mixtures for $CH_4/C_2H_6/C_3H_8$, the breakthrough time for C_2H_6 is almost maintained and the breakthrough time for C_3H_8 slightly decreases (Figure 5d). In addition, the captured C_3H_8 in the column can then be recovered with high purity during the regeneration desorption step. The desorption experiments at 298 K are further conducted to determine the recovery and productivity of C_3H_8. As revealed by Figure S6, CH_4 and C_2H_6 are removed within ca. 30 min·g^{-1} and 64.4 L·kg^{-1} high-purity (≥ 99.5%) C_3H_8 is obtained during the interim period (ca. 950 to 1180 min·g^{-1}). More importantly, gas flow and temperature also have no obvious influence on the high-purity C_3H_8 productivities (Figure 5e and f). To sum up, these excellent dynamic separation properties of HOF-NBDA make it a promising and accessible adsorbent for purified natural gas and recovery of C_3H_8 in the natural gas industry.

CONCLUSIONS

In summary, we report a stable layer HOF with hexagonal channels, which exhibits efficient $CH_4/C_2H_6/C_3H_8$ separation performance. Its C_3H_8 uptake at 5 kPa is as high as 52.2 cm^3·g^{-1}, and its IAST selectivities for CH_4/C_3H_8 (v/v, 85/15) and CH_4/C_2H_6 (v/v, 85/15) gas mixtures are 210.1 and 25.0 at 298 K and 100 kPa, respectively. The breakthrough experiments prove that HOF-NBDA can efficiently separate the $CH_4/C_2H_6/C_3H_8$ ternary mixture and produce high-purity CH_4 (70.9 L·kg^{-1}). In particularly, 54.2 L·kg^{-1} of C_3H_8 with a

https://doi.org/10.1021/cbe.4c00057
Chem Bio Eng. 2024, 1, 846−854

purity greater than 99.5% could be directly obtained through desorption recovery. Theoretical calculations indicate that the efficient separation performance of HOF-NBDA is attributed to the more weak-interactions between C_3H_8 molecule and the framework. More importantly, this material has excellent cyclic regeneration and maintains the same separation performance under various complex conditions, which is very important for the practical application in industry.

■ ASSOCIATED CONTENT

Supporting Information

The Supporting Information is available free of charge at https://pubs.acs.org/doi/10.1021/cbe.4c00057.

Additional experimental details, PXRD patterns, Q_{st} calculations, IAST selectivity calculations, desorption curves for ternary gas mixtures, and CH_4 and C_3H_8 productivities (PDF)

■ AUTHOR INFORMATION

Corresponding Author

Mingyan Wu − *State Key Laboratory of Structure Chemistry, Fujian Institute of Research on the Structure of Matter, Chinese Academy of Sciences, Fuzhou, Fujian 350002, P. R. China; Fujian College, University of Chinese Academy of Sciences, Fuzhou, Fujian 350002, P. R. China; University of Chinese Academy of Sciences, Beijing 100049, P. R. China;* orcid.org/0000-0003-2610-285X; Email: wumy@fjirsm.ac.cn

Authors

Yunzhe Zhou − *State Key Laboratory of Structure Chemistry, Fujian Institute of Research on the Structure of Matter, Chinese Academy of Sciences, Fuzhou, Fujian 350002, P. R. China; Fujian College, University of Chinese Academy of Sciences, Fuzhou, Fujian 350002, P. R. China; University of Chinese Academy of Sciences, Beijing 100049, P. R. China*

Yongqin Zhu − *State Key Laboratory of Structure Chemistry, Fujian Institute of Research on the Structure of Matter, Chinese Academy of Sciences, Fuzhou, Fujian 350002, P. R. China*

Danhua Song − *State Key Laboratory of Structure Chemistry, Fujian Institute of Research on the Structure of Matter, Chinese Academy of Sciences, Fuzhou, Fujian 350002, P. R. China*

Zhenyu Ji − *State Key Laboratory of Structure Chemistry, Fujian Institute of Research on the Structure of Matter, Chinese Academy of Sciences, Fuzhou, Fujian 350002, P. R. China*

Cheng Chen − *State Key Laboratory of Structure Chemistry, Fujian Institute of Research on the Structure of Matter, Chinese Academy of Sciences, Fuzhou, Fujian 350002, P. R. China*

Complete contact information is available at: https://pubs.acs.org/10.1021/cbe.4c00057

Notes

The authors declare no competing financial interest.

■ ACKNOWLEDGMENTS

This work is supported by NSFC (22271282) and the Self-deployment Project Research Program of Haixi Institutes, Chinese Academy of Sciences with the grant number of CXZX-2022-JQ04. Additionally, this work is also supported by Fujian Science & Technology Innovation Laboratory for Optoelectronic Information of China (No. 2021ZR120) and NSF of Fujian Province (No. 2021J01517 and 2020J06034).

■ REFERENCES

(1) Nugent, P.; Belmabkhout, Y.; Burd, S. D.; Cairns, A. J.; Luebke, R.; Forrest, K.; Pham, T.; Ma, S.; Space, B.; Wojtas, L.; Eddaoudi, M.; Zaworotko, M. J. Porous Materials with Optimal Adsorption Thermodynamics and Kinetics for CO_2 Separation. *Nature* **2013**, *495* (7439), 80−84.

(2) Lu, J.; Cao, R. Porous Organic Molecular Frameworks with Extrinsic Porosity: A Platform for Carbon Storage and Separation. *Angew. Chem. Int. Ed.* **2016**, *55* (33), 9474−9480.

(3) Dinakar, B.; Forse, A. C.; Jiang, H. Z. H.; Zhu, Z.; Lee, J.-H.; Kim, E. J.; Parker, S. T.; Pollak, C. J.; Siegelman, R. L.; Milner, P. J.; Reimer, J. A.; Long, J. R. Overcoming Metastable CO_2 Adsorption in a Bulky Diamine-Appended Metal-Organic Framework. *J. Am. Chem. Soc.* **2021**, *143* (37), 15258−15270.

(4) Liang, W.; Bhatt, P. M.; Shkurenko, A.; Adil, K.; Mouchaham, G.; Aggarwal, H.; Mallick, A.; Jamal, A.; Belmabkhout, Y.; Eddaoudi, M. A Tailor-Made Interpenetrated MOF with Exceptional Carbon-Capture Performance from Flue Gas. *Chem.* **2019**, *5* (4), 950−963.

(5) Evans, H. A.; Mullangi, D.; Deng, Z.; Wang, Y.; Peh, S. B.; Wei, F.; Wang, J.; Brown, C. M.; Zhao, D.; Canepa, P.; Cheetham, A. K. Aluminum formate, $Al(HCOO)_3$: An Earth-Abundant, Scalable, and Highly Selective Material for CO_2 Capture. *Sci. Adv.* **2022**, *8* (44) DOI: 10.1126/sciadv.ade1473.

(6) Alvarez, R. A.; Zavala-Araiza, D.; Lyon, D. R.; Allen, D. T.; Barkley, Z. R.; Brandt, A. R.; Davis, K. J.; Herndon, S. C.; Jacob, D. J.; Karion, A.; Kort, E. A.; Lamb, B. K.; Lauvaux, T.; Maasakkers, J. D.; Marchese, A. J.; Omara, M.; Pacala, S. W.; Peischl, J.; Robinson, A. L.; Shepson, P. B.; Sweeney, C.; Townsend-Small, A.; Wofsy, S. C.; Hamburg, S. P. Assessment of Methane Emissions from the US Oil and Gas Supply Chain. *Science* **2018**, *361* (6398), 186−188.

(7) Brandt, A. R.; Heath, G. A.; Kort, E. A.; O'Sullivan, F.; Petron, G.; Jordaan, S. M.; Tans, P.; Wilcox, J.; Gopstein, A. M.; Arent, D.; Wofsy, S.; Brown, N. J.; Bradley, R.; Stucky, G. D.; Eardley, D.; Harriss, R. Methane Leaks from North American Natural Gas Systems. *Science* **2014**, *343* (6172), 733−735.

(8) Cao, Z.-M.; Li, G.-L.; Di, Z.-Y.; Chen, C.; Meng, L.-Y.; Wu, M.; Wang, W.; Zhuo, Z.; Kong, X.-J.; Hong, M.; Huang, Y.-G. From a Metal-Organic Square to a Robust and Regenerable Supramolecular Self-assembly for Methane Purification. *Angew. Chem. Int. Ed.* **2022**, *61* (48), No. e202210012.

(9) Chen, Y.; Jiang, Y.; Li, J.; Hong, X.; Ni, H.; Wang, L.; Ma, N.; Tong, M.; Krishna, R.; Zhang, Y. Optimizing the Cask Effect in Multicomponent Natural Gas Purification to Provide High Methane Productivity. *AIChE J.* **2024**, *70* (3), No. e18320.

(10) Cai, Y.; Chen, H.; Liu, P.; Chen, J.; Xu, H.; Alshahrani, T.; Li, L.; Chen, B.; Gao, J. Robust Microporous Hydrogen-Bonded Organic Framework for Highly Selective Purification of Methane from Natural gas. *Micropor. Mesopor. Mater.* **2023**, *352*, 112495.

(11) Deng, C.; Zhao, L.; Gao, M.-Y.; Darwish, S.; Song, B.-Q.; Sensharma, D.; Lusi, M.; Peng, Y.-L.; Mukherjee, S.; Zaworotko, M. J. Ultramicroporous Lonsdaleite Topology MOF with High Propane Uptake and Propane/Methane Selectivity for Propane Capture from Simulated Natural Gas. *ACS Mater. Lett.* **2024**, *6* (1), 56−65.

(12) Qin, L.-Z.; Xiong, X.-H.; Wang, S.-H.; Zhang, L.; Meng, L.-L.; Yan, L.; Fan, Y.-N.; Yan, T.-A.; Liu, D.-H.; Wei, Z.-W.; Su, C.-Y. MIL-101-Cr/Fe/Fe-NH_2 for Efficient Separation of CH_4 and C_3H_8 from Simulated Natural Gas. *ACS Appl. Mater. Interfaces* **2022**, *14* (40), 45444−45450.

(13) Lan, L.; Lu, N.; Yin, J.-C.; Gao, Q.; Lang, F.; Zhang, Y.-H.; Nie, H.-X.; Li, N.; Bu, X.-H. Simultaneous Extraction of C_3H_8 and C_2H_6 from Ternary $C_3H_8/C_2H_6/CH_4$ Mixtures in an Ultra-Microporous Metal-Organic Framework. *Chem. Eng. J.* **2023**, *476* (15), 146750.

(14) Zeng, H.; Xie, M.; Wang, T.; Wei, R.-J.; Xie, X.-J.; Zhao, Y.; Lu, W.; Li, D. Orthogonal-Array Dynamic Molecular Sieving of Propylene/Propane Mixtures. *Nature* **2021**, *595* (7868), 542−548.
(15) Cui, J.; Zhang, Z.; Yang, L.; Hu, J.; Jin, A.; Yang, Z.; Zhao, Y.; Meng, B.; Zhou, Y.; Wang, J.; Su, Y.; Wang, J.; Cui, X.; Xing, H. A Molecular Sieve with Ultrafast Adsorption Kinetics for Propylene Separation. *Science* **2024**, *383* (6679), 179−183.
(16) Huang, Y.; Wan, J.; Pan, T.; Ge, K.; Guo, Y.; Duan, J.; Bai, J.; Jin, W.; Kitagawa, S. Delicate Softness in a Temperature-Responsive Porous Crystal for Accelerated Sieving of Propylene/Propane. *J. Am. Chem. Soc.* **2023**, *145* (44), 24425−24432.
(17) Zhou, Y.; Chen, C.; Krishna, R.; Ji, Z.; Yuan, D.; Wu, M. Tuning Pore Polarization to Boost Ethane/Ethylene Separation Performance in Hydrogen-Bonded Organic Frameworks. *Angew. Chem. Int. Ed.* **2023**, *62* (25), No. e202305041.
(18) Di, Z.; Liu, C.; Pang, J.; Zou, S.; Ji, Z.; Hu, F.; Chen, C.; Yuan, D.; Hong, M.; Wu, M. A Metal-Organic Framework with Nonpolar Pore Surfaces for the One-step Acquisition of C_2H_4 from a C_2H_4 and C_2H_6 Mixture. *Angew. Chem. Int. Ed.* **2022**, *61* (42), No. e202210343.
(19) Bao, Z.; Chang, G.; Xing, H.; Krishna, R.; Ren, Q.; Chen, B. Potential of Microporous Metal-Organic Frameworks for Separation of Hydrocarbon Mixtures. *Energy Environ. Sci.* **2016**, *9* (12), 3612−3641.
(20) Lin, R.-B.; Xiang, S.; Zhou, W.; Chen, B. Microporous Metal-Organic Framework Materials for Gas Separation. *Chem.* **2020**, *6* (2), 337−363.
(21) Adil, K.; Bhatt, P. M.; Belmabkhout, Y.; Abtab, S. M. T.; Jiang, H.; Assen, A. H.; Mallick, A.; Cadiau, A.; Aqil, J.; Eddaoudi, M. Valuing Metal-Organic Frameworks for Postcombustion Carbon Capture: A Benchmark Study for Evaluating Physical Adsorbents. *Adv. Mater.* **2017**, *29* (39), 1702953.
(22) Lin, R.-B.; Zhang, Z.; Chen, B. Achieving High Performance Metal-Organic Framework Materials through Pore Engineering. *Acc. Chem. Res.* **2021**, *54* (17), 3362−3376.
(23) Yamane, Y.; Miyahara, M. T.; Tanaka, H. High-Performance Carbon Molecular Sieves for the Separation of Propylene and Propane. *ACS Appl. Mater. Interfaces* **2022**, *14* (15), 17878−17888.
(24) Di, Z.; Liu, C.; Pang, J.; Chen, C.; Hu, F.; Yuan, D.; Wu, M.; Hong, M. Cage-Like Porous Materials with Simultaneous High C_2H_2 Storage and Excellent C_2H_2/CO_2 Separation Performance. *Angew. Chem. Int. Ed.* **2021**, *60* (19), 10828−10832.
(25) Li, H.; Liu, C.; Chen, C.; Di, Z.; Yuan, D.; Pang, J.; Wei, W.; Wu, M.; Hong, M. An Unprecedented Pillar-Cage Fluorinated Hybrid Porous Framework with Highly Efficient Acetylene Storage and Separation. *Angew. Chem. Int. Ed.* **2021**, *60* (14), 7547−7552.
(26) Zhang, P.; Wen, X.; Wang, L.; Zhong, Y.; Su, Y.; Zhang, Y.; Wang, J.; Yang, J.; Zeng, Z.; Deng, S. Algae-Derived N-Doped Porous Carbons with Ultrahigh Specific Surface Area for Highly Selective Separation of Light Hydrocarbons. *Chem. Eng. J.* **2020**, *381* (1), 122731.
(27) Song, X.; Wang, Y.; Wang, C.; Wang, D.; Zhuang, G.; Kirlikovali, K. O.; Li, P.; Farha, O. K. Design Rules of Hydrogen-Bonded Organic Frameworks with High Chemical and Thermal Stabilities. *J. Am. Chem. Soc.* **2022**, *144* (24), 10663−10687.
(28) Xi, X.-J.; Li, Y.; Lang, F.-F.; Xu, L.; Pang, J.; Bu, X.-H. Robust Porous Hydrogen-Bonded Organic Frameworks: Synthesis and Applications in Gas Adsorption and Separation. *Giant* **2023**, *16*, 100181.
(29) Hu, F.; Liu, C.; Wu, M.; Pang, J.; Jiang, F.; Yuan, D.; Hong, M. An Ultrastable and Easily Regenerated Hydrogen-Bonded Organic Molecular Framework with Permanent Porosity. *Angew. Chem. Int. Ed.* **2017**, *56* (8), 2101−2104.
(30) Zhang, X.; Li, L.; Wang, J.-X.; Wen, H.-M.; Krishna, R.; Wu, H.; Zhou, W.; Chen, Z.-N.; Li, B.; Qian, G.; Chen, B. Selective Ethane/Ethylene Separation in a Robust Microporous Hydrogen-Bonded Organic Framework. *J. Am. Chem. Soc.* **2020**, *142* (1), 633−640.
(31) Yang, Y.; Zhang, H.; Yuan, Z.; Wang, J.-Q.; Xiang, F.; Chen, L.; Wei, F.; Xiang, S.; Chen, B.; Zhang, Z. An Ultramicroporous Hydrogen-Bonded Organic Framework Exhibiting High C_2H_2/CO_2 Separation. *Angew. Chem. Int. Ed.* **2022**, *61* (43), No. e202207579.
(32) He, Y.; Xiang, S.; Chen, B. A Microporous Hydrogen-Bonded Organic Framework for Highly Selective C_2H_2/C_2H_4 Separation at Ambient Temperature. *J. Am. Chem. Soc.* **2011**, *133* (37), 14570−14573.
(33) Chen, Y.; Yang, Y.; Wang, Y.; Xiong, Q.; Yang, J.; Xiang, S.; Li, L.; Li, J.; Zhang, Z.; Chen, B. Ultramicroporous Hydrogen-Bonded Organic Framework Material with a Thermoregulatory Gating Effect for Record Propylene Separation. *J. Am. Chem. Soc.* **2022**, *144* (37), 17033−17040.
(34) Willems, T. F.; Rycroft, C. H.; Kazi, M.; Meza, J. C.; Haranczyk, M. Algorithms and tools for high-throughput geometry-based analysis of crystalline porous materials. *Micropor. Mesopor. Mater.* **2012**, *149* (1), 134−141.
(35) Zhang, X.-X.; Guo, X.-Z.; Chen, S.-S.; Kang, H.-W.; Zhao, Y.; Gao, J.-X.; Xiong, G.-Z.; Hou, L. A Stable Microporous Framework with Multiple Accessible Adsorption Sites for High Capacity Adsorption and Efficient Separation of Light Hydrocarbons. *Chem. Eng. J.* **2023**, *466* (15), 143170.
(36) Zhang, L.; Xiong, X.-H.; Meng, L.-L.; Qin, L.-Z.; Chen, C.-X.; Wei, Z.-W.; Su, C.-Y. Engineering Pore Nanospaces by Introducing Aromatic Effects in UiO-66 for Efficient Separation of Light Hydrocarbons. *J. Mater. Chem. A* **2023**, *11* (24), 12902−12909.
(37) Shi, X.; Zu, Y.; Li, X.; Zhao, T.; Ren, H.; Sun, F. Highly Selective Adsorption of Light Hydrocarbons in a HKUST-like MOF Constructed from Spirobifluorene-Based Octacarboxylate Ligand by a Substitution Strategy. *Nano Res.* **2023**, *16* (7), 10652−10659.
(38) Zhao, L.; Liu, P.; Deng, C.; Wang, T.; Wang, S.; Tian, Y.-J.; Zou, J.-S.; Wu, X.-C.; Zhang, Y.; Peng, Y.-L.; Zhang, Z.; Zaworotko, M. J. Robust ultra-microporous metal-organic frameworks for highly efficient natural gas purification. *Nano Res.* **2023**, *16* (10), 12338−12344.
(39) Liu, Y.; Xu, Q.; Chen, L.; Song, C.; Yang, Q.; Zhang, Z.; Lu, D.; Yang, Y.; Ren, Q.; Bao, Z. Hydrogen-bonded metal-nucleobase frameworks for highly selective capture of ethane/propane from methane and methane/nitrogen separation. *Nano Res.* **2022**, *15* (8), 7695−7702.
(40) Yuan, Y.; Wu, H.; Xu, Y.; Lv, D.; Tu, S.; Wu, Y.; Li, Z.; Xia, Q. Selective extraction of methane from C1/C2/C3 on moisture-resistant MIL-142A with interpenetrated networks. *Chem. Eng. J.* **2020**, *395* (1), 125057.
(41) Zhang, Y.; Xiao, H.; Zhou, X.; Wang, X.; Li, Z. Selective Adsorption Performances of UiO-67 for Separation of Light Hydrocarbons C1, C2, and C3. *Ind. Eng. Chem. Res.* **2017**, *56* (30), 8689−8696.
(42) Wang, Y.; Lai, Y.; Liu, J.; Fan, Z.; Quan, X.; Zhang, T.; Wang, C.; Xu, C.; Chen, Q.; Niu, Z. A Zn-Cluster-Based MOF for Efficient Separation of $C_3H_8/C_2H_6/CH_4$. *Chem. Bio. Eng.* **2024**, DOI: 10.1021/cbe.3c00092.
(43) Lin, D. X.; Tu, S.; Yu, L.; Yuan, Y. N.; Wu, Y.; Zhou, X.; Li, Z.; Xia, Q. B. Highly Efficient Separation of $CH_4/C_2H_6/C_3H_8$ from Natural Gas on a Novel Copper-Based Metal-Organic Framework. *Ind. Eng. Chem. Res.* **2023**, *62* (12), 5252−5261.
(44) Song, Z.; Zheng, Y.; Chen, Y.; Cai, Y.; Wei, R.-J.; Gao, J. Halogen-Modified Metal-Organic Frameworks for Efficient Separation of Alkane from Natural Gas. *Dalton Trans.* **2023**, *52* (42), 15462−15466.
(45) Wang, L.; Zhang, W.; Ding, J.; Gong, L.; Krishna, R.; Ran, Y.; Chen, L.; Luo, F. Th-MOF showing six-fold imide-sealed pockets for middle-size-separation of propane from natural gas. *Nano Res.* **2023**, *16* (2), 3287−3293.
(46) Wang, G.-D.; Krishna, R.; Li, Y.-Z.; Ma, Y.-Y.; Hou, L.; Wang, Y.-Y.; Zhu, Z. Rational Construction of Ultrahigh Thermal Stable MOF for Efficient Separation of MTO Products and Natural Gas. *ACS Materials Lett.* **2023**, *5* (4), 1091−1099.
(47) Lysova, A. A.; Kovalenko, K. A.; Nizovtsev, A. S.; Dybtsev, D. N.; Fedin, V. P. Efficient separation of methane, ethane and propane

on mesoporous metal-organic frameworks. *Chem. Eng. J.* **2023**, *453* (1), 139642.
(48) Zhang, Y.; Yang, L.; Wang, L.; Duttwyler, S.; Xing, H. A Microporous Metal-Organic Framework Supramolecularly Assembled from a Cu(II) Dodecaborate Cluster Complex for Selective Gas Separation. *Angew.Chem. Int.Ed.* **2019**, *58* (24), 8145−8150.
(49) Liu, Y.; Li, H.; Zou, S.; Di, Z.; Chen, C.; Wu, M.; Hong, M. Exceptionally Water-Stable In(III)-Based Framework with Conjugated Rhombohedral Cavities for Efficiently Separating Humid Flue Gas. *ACS Sustainable Chem. Eng.* **2022**, *10* (46), 15335−15343.
(50) Xie, X.-J.; Zeng, H.; Xie, M.; Chen, W.; Hua, G.-F.; Lu, W.; Li, D. A Metal-Organic Framework for C_2H_2/CO_2 Separation under Highly Humid Conditions: Balanced Hydrophilicity/Hydrophobicity. *Chem. Eng. J.* **2022**, *427* (1), 132033.
(51) Gan, L.; Andres-Garcia, E.; Minguez Espallargas, G.; Planas, J. G. Adsorptive Separation of CO_2 by a Hydrophobic Carborane-Based Metal-Organic Framework under Humid Conditions. *ACS Appl. Mater. Interfaces.* **2023**, *15* (4), 5309−5316.

https://doi.org/10.1021/cbe.4c00057
Chem Bio Eng. 2024, 1, 846−854